

$H\cdots O < R_{\text{bnd}}$  and  $O-H > R_{\text{bnd}}$ ; some moderate extrapolation could, perhaps, be done at the other end of this range.

We thank I. D. Brown for kindly showing us the text with equation (5) before publication. This research has been supported by MPI and CNR grants.

#### References

- BAUR, W. H. (1970). *Trans. Am. Crystallogr. Assoc.* **6**, 123–155.  
 BERGERHOFF, G., HUNDT, R., SIEVES, R. & BROWN, I. D. (1983). *J. Chem. Inf. Comput. Sci.* **23**, 66–69.  
 BROWN, I. D. (1976a). *Acta Cryst.* **A32**, 24–31.

- BROWN, I. D. (1976b). *Acta Cryst.* **A32**, 786–792.  
 BROWN, I. D. (1981). *Structures and Bonding*, Vol. 2, edited by M. O'KEEFE & M. NAVROTSKY. New York: Academic Press.  
 BROWN, I. D. (1987). *Phys. Chem. Miner.* **15**, 30–34.  
 BROWN, I. D. & ALTERMATT, D. (1985). *Acta Cryst.* **B41**, 244–247.  
 BROWN, I. D. & WU, K. K. (1976). *Acta Cryst.* **B32**, 1957–1959.  
 CHIARI, G. & FERRARIS, G. (1982). *Acta Cryst.* **B38**, 2331–2341.  
 FERRARIS, G. & FRANCHINI-ANGELA, M. (1972). *Acta Cryst.* **B28**, 3572–3583.  
 FERRARIS, G., FUESS, H. & JOSWIG, W. (1986). *Acta Cryst.* **B42**, 253–258.  
 FERRARIS, G. & IVALDI, G. (1984). *Acta Cryst.* **B40**, 1–6.  
 FERRARIS, G. & IVALDI, G. (1987). *Acta Cryst.* **A43**, C76.  
 ISHIKAWA, M. (1978). *Acta Cryst.* **B34**, 2074–2080.  
 JOSWIG, W., FUESS, H. & FERRARIS, G. (1982). *Acta Cryst.* **B38**, 2798–2801.  
 PAULING, L. (1929). *J. Am. Chem. Soc.* **51**, 1010–1026.

*Acta Cryst.* (1988). **B44**, 344–351

## The Incommensurately Modulated Structure of an Andesine ( $An_{38}$ )

BY W. STEURER AND H. JAGODZINSKI

*Institut für Kristallographie und Mineralogie der Universität, Theresienstraße 41, D-8000 München 2, Federal Republic of Germany*

(Received 4 October 1987; accepted 15 February 1988)

*Dedicated to Professor Dr Theo Hahn on the occasion of his 60th birthday*

#### Abstract

The modulated structure of the intermediate plagioclase  $Ca_{0.38}Na_{0.62}Al_{1.38}Si_{2.62}O_8$  has been determined by single-crystal X-ray methods. The structure has been refined using general sinusoidal density and displacement waves because only main reflections and first-order satellites were observable. Crystal data:  $M_r = 268.4$ , superspace group  $P_1^{P1}$  [0.080 (9), 0.031 (8), -0.261 (10)] with additional centering translations,  $a = 8.151$  (3),  $b = 12.829$  (5),  $c = 14.206$  (7) Å,  $\alpha = 93.62$  (3),  $\beta = 116.21$  (2),  $\gamma = 89.70$  (2)°,  $V = 1329.7$  Å<sup>3</sup>,  $Z = 8$ ,  $D_x = 2.68$  Mg m<sup>-3</sup>,  $Mo K\alpha$ ,  $\lambda = 0.71069$  Å,  $\mu = 1.03$  mm<sup>-1</sup>,  $F(000) = 980.9$ , half-period of the modulation wave  $T = 26.7$  (3) Å,  $wR = 0.047$  for all reflections, 0.044 for 1176 main reflections and 0.151 for 2343 satellite reflections. The analysis of the mean  $T$ -O bond lengths reveals nearly complete Al/Si ordering on the  $T$  sites. The displacive modulation of the extra framework cations is strongly correlated with the periodic distortion of the framework structure. There is no Ca/Na substitutional modulation. The long-range order of the modulated structure can be characterized by the sequence ...An...An\*... where An and An\* represent regions with  $I$ -anorthite-like structure having antiphase relation to each other. The disordered boundary zones ... correspond to the

average structure of the andesine. The absence of  $f$  reflections even in strongly overexposed X-ray diffraction photographs excludes any long-range order of anorthite- and albite-like lamellae as can be found in Ca-rich intermediate plagioclases.

#### Introduction

The diffraction patterns of intermediate plagioclases are characterized by numerous diffuse and/or sharp satellite reflections and diffuse scattering phenomena (Jagodzinski, 1984). They reflect complicated structures resulting from complex ordering and/or exsolution processes dependent on chemical composition and conditions of formation. Their most prominent feature besides the main reflections are the  $e$  and, in Ca-rich plagioclases, the  $f$  reflections. They can be interpreted as first- and second-order satellites caused by Al/Si and Ca/Na ordering ( $a$  or main reflections  $hkl0$ :  $h + k = 2n$ ,  $l = 2n$ ;  $e$  satellites  $hkml$ :  $h + k = 2n + 1$ ,  $l = 2n + 1$ ,  $m = \pm 1$ ;  $f$  satellites  $hkml$ :  $h + k = 2n$ ,  $l = 2n$ ,  $m = \pm 2$ ). Electron diffraction patterns, with their enhancement of weak satellite reflections resulting from dynamical scattering, even show third-order satellites [for  $An_{52}$  see Nakajima, Morimoto & Kitamura (1977)] indicating a rather high coherence

Table 1. *R* factors of X-ray structure determinations of *e*-plagioclases

An <sub>73</sub>	Kitamura & Morimoto (1975, 1977), <i>R</i> = 0.31 (210 <i>a</i> and <i>e</i> reflections) and 0.24 (all reflections with <i>I</i> > 0) for 132 variables
An <sub>55</sub>	Toman & Frueh (1976 <i>a,b</i> ), <i>R</i> = 0.071 (720 <i>a</i> ), 0.215 (492 <i>e</i> ) and 0.27 (318 <i>f</i> reflections) for 307 variables
An <sub>52</sub>	Horst, Tagai, Korekawa & Jagodzinski (1981), <i>R</i> = 0.08 (4910 <i>a</i> and <i>e</i> ), 0.066 (1640 <i>a</i> ) and 0.182 (3270 <i>e</i> reflections) for 255 variables
An <sub>52</sub>	Yamamoto, Nakazawa, Kitamura & Morimoto (1984), <i>R</i> = 0.08 (4910 <i>a</i> and <i>e</i> ), 0.066 (1640 <i>a</i> ) and 0.105 (3220 <i>e</i> reflections) for 429 variables [same data set as Horst <i>et al.</i> (1981)]
An <sub>38</sub>	This work, <i>R</i> = 0.106, <i>wR</i> = 0.047 (3519 <i>a</i> and <i>e</i> ), <i>R</i> = 0.044, <i>wR</i> = 0.044 (1176 <i>a</i> ) and <i>R</i> = 0.33, <i>wR</i> = 0.151 (2343 <i>e</i> reflections) for 216 variables

length of the modulated structure and small phase fluctuations only.

From the interpretation of electron microscopic images, crystal-chemical considerations and more-or-less quantitative X-ray structure analyses (Table 1), different structure models of the *e*-plagioclases have been derived [for a review see Kitamura & Morimoto (1984)]. In spite of the modulation period varying strongly with composition [from 40 to 140 Å; Ribbe, 1983] and the definite change of properties at about An<sub>50</sub> (Carpenter, 1986) validity of the respective models has been claimed for the whole range of *e*-plagioclase compositions.

The main difference between the more recent models lies in the Ca/Na ordering. According to the KM (Kitamura & Morimoto, 1977) model the modulated structure can be described by a sequence of lamellae with An-like structure separated by lamellae with Ab-like structure: An...Ab...An\*. The HTKJ (Horst, Tagai, Korekawa & Jagodzinski, 1981) model gives similar Al/Si and Ca/Na ordering for Ca-rich plagioclases but describes the more sodic ones by the sequence: An...An\*...An. The applicability of the KM model to Ca-rich plagioclases has been shown by the semiquantitative X-ray structure determinations performed on a bytownite from the Huttenlocher miscibility gap (Kitamura & Morimoto, 1975, 1977). Both strong Al/Si and Ca/Na substitutional modulation has been found. The results of the structure determination of a labradorite from the Bøggild exsolution (Yamamoto, Nakazawa, Kitamura & Morimoto, 1984), however, are in accordance with both models because the *f* satellites, which are necessary for discrimination between the models, had not been included in the refinements.

It should be kept in mind that an X-ray structure analysis of an intermediate plagioclase can only give an average modulated structure if diffraction phenomena like supersatellites or diffuse scattering are neglected. No information about short-range order will be available as can be obtained from electron microscope studies. The present work has been undertaken to obtain information about the real structure of a more

sodic plagioclase. The andesine crystal studied has the advantage of being chemically homogenous. The crystals mentioned above stem from miscibility gaps and do not allow correct structure determinations because of the incoherent superposition of the respective *a* and *e* reflections of both the end members of the exsolution gap.

### Experimental

The single crystal used for intensity data collection is a regionally metamorphic andesine. It originates from an andesine (An<sub>38</sub>)–labradorite (An<sub>63</sub>) intergrowth from Gordemo, Verzasca Valley. The crystal, Vz433, was described in detail by Wenk, Joswig, Tagai, Korekawa & Smith (1980) and Smith & Wenk (1983).

Data collection: Enraf–Nonius CAD-4 four-circle diffractometer, graphite monochromator, Mo *K*α, ω/2θ scans; one intensity control measurement per hour, stable within counting statistics; three orientation control reflections every 50 measured reflections; θ<sub>max</sub> = 30°; main reflections measured with prescans, satellites with a constant scan time of 2 min each; −8 ≤ *h* ≤ 8, −15 ≤ *k* ≤ 15, 0 ≤ *l* ≤ 16, −1 ≤ *m* ≤ 1; 3521 reflections (1178 *a* and 2343 *e*), 1999 (1055 *a* and 944 *e*) with *I* > 2σ(*I*); (0,14,2,0) and (0040) rejected because of incoherent superposition of supersatellites. Lp correction, no absorption correction (μ = 1.03 mm<sup>−1</sup>).

Before data collection the crystal was investigated extensively by X-ray film methods to find *f* satellites. On special precession photographs (crystal-to-film distance 100 mm, Cu *K*α) the weak *e* satellite (1̄031) could be observed but not the *f* reflection (0002). Small-angle-scattering photographs show a higher intensity for this *f* satellite than for the *e* reflection for An<sub>70</sub> and comparable intensities for An<sub>52</sub> (Jagodzinski 1984, 1986). *f* reflections were also not observed in strongly overexposed rotation photographs (around [0010]). Besides sharp *a* and *e* reflections and some diffuse streaks crossing *a* reflections, supersatellites with different *q* vectors could be observed around some main reflections such as (2̄040) and (0040).

### (3+1)-Dimensional Patterson function, (3+1)-PF

According to the approach of de Wolff (1974) one-dimensionally modulated structures can be described in a fictitious (3+1)-dimensional lattice. Thereby the translational symmetry lost in the three-dimensional space is restored. The (3+1)-dimensional unit cell contains the atoms as continuous strings ('string atoms') with the shape of the modulation function in the extra dimension *t*. The (3+1)-PF is the vector function between these 'string atoms' as the conventional Patterson function is between 'ordinary' atoms. The (3+1)-PF is centrosymmetric and con-

tinuous in the extra dimension (Steurer, 1987). Fig. 1 illustrates schematically a (1+1)-dimensional cell with 'string atoms' in  $x_1$  and  $x_2$ . The (1+1)-PF for a vector set with a particular  $T = \Delta t$  is proportional to the number of equivalent vectors ( $\Delta x$ ,  $\Delta t$ ) between the 'string atoms'. From the position of the maximum at  $U = \Delta r_{kk'}$  (the Patterson vector between the 'ordinary' atoms of the basic structure) and  $T = \Delta t = -\Delta\phi_{kk'}$ , the phase difference between the modulation functions can be derived. In the case of displacive modulation the 'bordering peaks' at  $U = \Delta r_{kk'} \pm (A_k + A_{k'})$  and  $T = \Delta t + 0.5$  give the amplitude sums  $A_k + A_{k'}$ .

The magnitudes of the displacement waves can be estimated from the values of the anisotropic temperature-factor coefficients of the average structure. Accordingly, the amplitudes for the framework atoms could be expected to amount to 0.1 Å and for the Ca/Na positions to about 0.4 Å. Therefore it can be expected that the structure refinements should converge well once reasonable starting values for the Ca/Na modulation have been found. This would be a consequence of the linear dependence of the structure factor on the amplitudes if they are small enough, and of the assumption that the modulation waves of all atoms had similar phases in an antiphase domain structure.

Fig. 2 represents sections of the (3+1)-PF of the interaction  $M-M^c$  ( $M$  stands for the Ca/Na site and  $M^c$  for the position generated by the centre of symmetry from  $M$ ). The modulation waves of atoms connected by a centre of symmetry  $c$  have the amplitude sum  $(A_k + A_{k'}) = 2A_k$  and the phase difference  $\Delta\phi_{kk'} =$

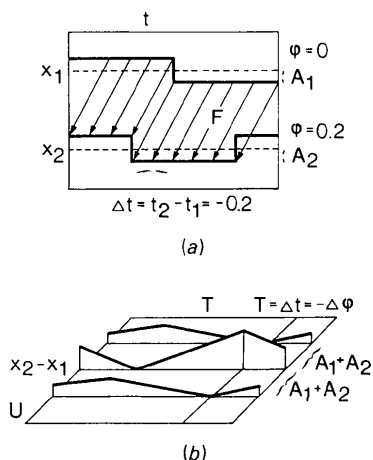


Fig. 1. (a) Schematic drawing of a (1+1)-dimensional unit cell with two rectangularly shift-modulated point atoms in  $x_1$  and  $x_2$ . The 'string atoms' have a phase difference  $\Delta\phi = 0.2$ . The number of equivalent vectors between the 'string atoms' is proportional to the area  $F$  and depends on  $\Delta t$  (maximal for vectors with components  $\Delta t = \Delta\phi$ ). The shape of this vector function is (1+1)-PF and is illustrated in (b). The maximum in  $U = x_2 - x_1$  is at  $T = -\Delta\phi$ . The 'bordering maxima' in  $T + 0.5$  and  $U = x_2 - x_1 \pm (A_1 + A_2)$  give the amplitude sums.

$\phi_k - (-\phi_k) = 2\phi_k$ . From Fig. 2 we find from the positions of the maximum at  $\mathbf{R} = \Delta\mathbf{r}_{M-M^c}$  ( $U = 0.54$ ,  $V = 0$ ,  $W = 0.14$ ) and of the 'bordering peaks' ( $U = 0.54$ ,  $V = -0.08$ ,  $W = 0.18$  and  $U = 0.54$ ,  $V = 0.08$ ,  $W = 0.10$ ) the amplitude sums  $2A_M^y = 0.08$  and  $2A_M^z = -0.04$ . Hence the amplitudes  $A_M^y = 0.04$  and  $A_M^z = -0.02$  follow. For the determination of the phase differences it is appropriate to analyse the (3+1)-PF in sections parallel to  $UT$ ,  $VT$  and  $WT$ . Fig. 3 shows the section parallel to  $VT$  and we easily derive the phase difference  $\Delta\phi_{M-M^c}^y$ . The maximum at  $\mathbf{R} = \Delta\mathbf{r}_{M-M^c}$  ( $V = 0$ ) is at  $T = 0.1 = -\Delta\phi_{M-M^c}^y = -2\phi_M^y$ . Hence  $\phi_M^y = 0.45$  or  $0.95$  follows. From the irregular shape of the peaks in Fig. 2 it can be inferred that the modulation of

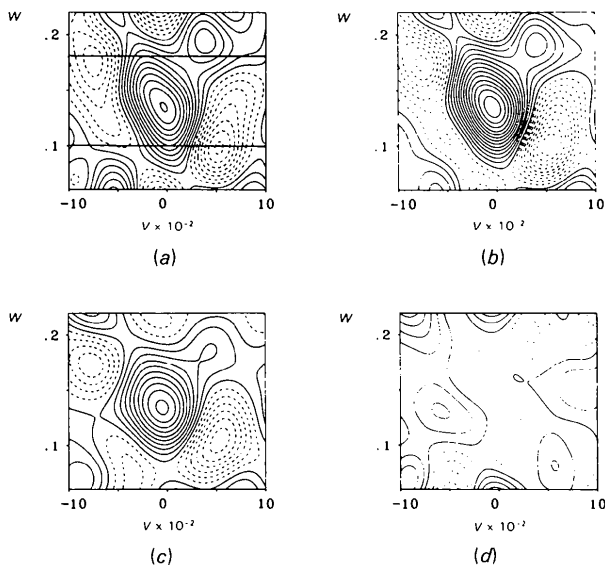


Fig. 2. Sections through the (3+1)-PF of  $\text{An}_{38}$  calculated with  $e$  reflections only. The region around the  $M-M^c$  vector is shown for: (a)  $T = 0$ , (b)  $T = 0.125$ , (c)  $T = 0.25$  and (d)  $T = 0.375$ . Dotted line: negative regions. The straight full lines in (a) mark the range for the bounded projection parallel to  $VT$  of Fig. 3.

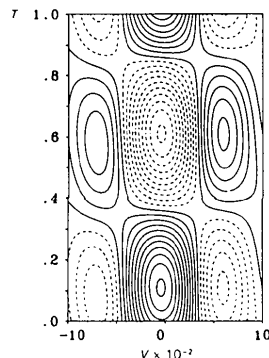


Fig. 3. Bounded projection of the (3+1)-PF of  $\text{An}_{38}$ , calculated with  $e$  satellites only. The region around the  $M-M^c$  interaction marked by straight lines in Fig. 2 is shown in a bounded projection with  $U = 0.54$  and  $0.10 \leq V \leq 0.18$ . Dotted lines: negative regions.

the  $M$  site has to be described by two split atoms both with density and shift modulation. In that case one can choose the starting values for the density waves:  $A_{M(1)}^p = 1$ ,  $\varphi_{M(1)}^p = 0.95$  and  $A_{M(2)}^p = 1$ ,  $\varphi_{M(2)}^p = 0.45$ . The parameters for the amplitudes and phases of the shift waves could then be arbitrary small starting values. In a similar way the interactions  $M-O_A(1)$ ,  $O_A(1)-T_1(O)$  and some others have been analysed using the (3+1)-PF.

### Structure refinement

The refinements have been carried out in the centrosymmetric triclinic superspace group  $P_1^{P1}$  with additional centring translations. A detailed discussion of the supersymmetry can be found, for example, in Yamamoto *et al.* (1984). The refinements started using general sinusoidal displacement waves  $\{A_k^x \sin[2\pi(\mathbf{q} \cdot \mathbf{r}_{kl} + \varphi_k^x)], A_k^y \sin[2\pi(\mathbf{q} \cdot \mathbf{r}_{kl} + \varphi_k^y)], A_k^z \sin[2\pi(\mathbf{q} \cdot \mathbf{r}_{kl} + \varphi_k^z)]\}$  for atoms  $k$  in the cell  $l$  for all atoms. The positional and thermal parameters were taken from the average structure (Wenk *et al.*, 1980). Amplitudes and phases were chosen according to the results of the (3+1)-PF or as arbitrary small values, respectively. The  $M$  site was described by one displacively modulated atom. This model converged smoothly to  $wR = 0.25$  for the  $e$  reflections.

After an analysis of the (3+1)-dimensional Fourier function [(3+1)-FF, *cf.* Steurer (1987)] the split-atom description mentioned above was introduced by refining independent density (occupancy factor  $p'_{kl}(\mathbf{q}, \mathbf{r}_{kl}) = p_k^0 \cdot 0.5 \{1 + A_k^z \sin[2\pi(\mathbf{q} \cdot \mathbf{r}_{kl} + \varphi_k^z)]\}$ ) and shift waves for each split site. The occupancy factors were fixed to the values obtained for the average structure ( $p_k^0$ ). Final  $R$  factors:  $R = 0.058$ ,  $wR = 0.047$ ,  $aR = 0.106$  for 1997 observed [ $I > 2\sigma(I)$ ] and 3519  $a$  and  $e$  reflections including the unobserved ones,  $R = 0.038$ ,  $wR = 0.044$ ,  $aR = 0.044$  for 1053 observed and totally 1176  $a$  reflections (as compared with  $R = 0.045$ ,  $wR = 0.043$  for the average structure),  $R = 0.161$ ,  $wR = 0.151$ ,  $aR = 0.334$  for 943 observed and totally 2343  $e$  satellites. To get a better feeling for the quality of the refinements  $F(\text{obs.})/F(\text{calc.})$  plots are given in Fig. 4. The distribution of structure factors is very similar for those  $a$  and  $e$  reflections which have been measured with comparable accuracy. The relatively large  $R$  factor for the satellites, therefore, is not only due to the deficiencies of the refined model but, primarily, due to counting statistics (the average relative satellite intensities are about two times higher for  $\text{An}_{52}$  than for  $\text{An}_{38}$ ). Structure-factor calculations for the second-order satellites are in full agreement with the non-observability of the  $f$  reflections with X-ray methods.

Refinements in the noncentrosymmetric superspace group  $P_1^{P1}$ , performed to examine the possibility of a noncentrosymmetric distribution of Ca and Na on the

$M$  sites (Jagodzinsky, 1984) did not give significantly lower  $R$  factors. To study the influence of structural changes in the antiphase domain boundaries, refinements using box-like modulation functions have been carried out. The results are similar, but the  $R$  factors are worse ( $wR = 0.207$  for the  $e$  reflections).

HRTEM photographs of sodium-rich  $e$ -plagioclases show regions with the modulated structure and parts with the  $C\bar{1}$  structure (Grove, Ferry & Spear, 1983). If the crystal used for our data collection exhibits similar coexistent structures, then the  $a$  reflections of the respective structures would coincide. To check this possibility refinements with different scale factors for  $a$  and  $e$  reflections have been performed. The  $R$  factor for the satellites decreased slightly from  $wR = 0.151$  to 0.148 and the amplitudes of the modulation waves increased nearly by a factor of two. The scale factor converged to the value 0.45. The correlations between this scale factor and the amplitudes are, of course, very high. If this scale factor is interpreted as a phason factor according to Overhauser (1971) [ $\exp(-1/2m^2 \times \langle \psi^2 \rangle)$ ] then  $\langle \psi^2 \rangle = 1.55$  corresponding to a phase fluctuation of  $\pm 20\%$  ( $\pm 72^\circ$ ). The weakening factor for the second-order satellites would consequently be 0.04.

An adapted version of the *Structure Determination Package (SDP)* (Frenz, 1978) was used for the refinements. It contains the structure-factor formula in analytical form as derived by Steurer & Adlhart (1983). The weighted  $R$  factor was minimized, the weights of the reflections were proportional to  $1/\sigma^2(I)$ . Atomic

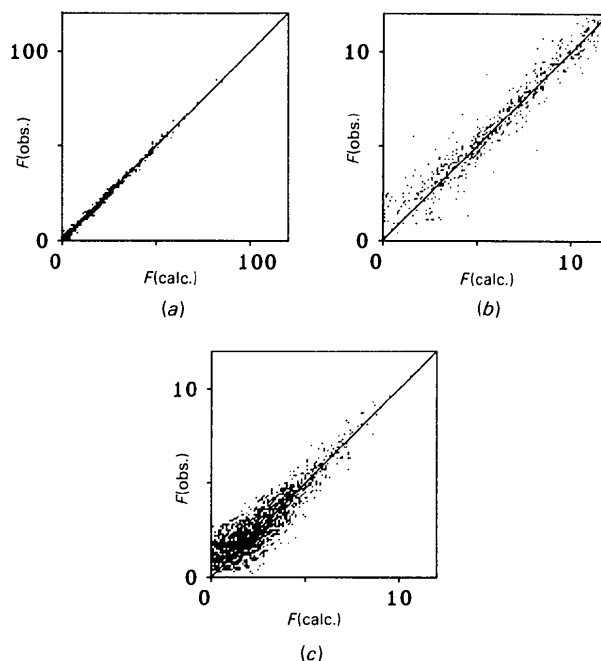


Fig. 4.  $F(\text{obs.})/F(\text{calc.})$  plots for (a) the main reflections, (b) part of (a) magnified ten times and (c) the satellite reflections on the same scale as (b).

Table 2. Fractional atomic coordinates ( $\times 10^4$ ), equivalent isotropic thermal parameters ( $\text{\AA}^2 \times 10^3$ ), amplitudes in fractions of  $a$ ,  $b$ ,  $c$  ( $\times 10^3$ ) and phases in fractions of one period ( $\times 10^2$ ) of the shift waves

E.s.d.'s in parentheses.  $U_{\text{eq}} = \frac{1}{3}(U_{11} + U_{22} + U_{33})$ . Occupancy factors:  $M(1) = 0.18$  (1)Ca +  $0.29$  (1)Na,  $M(2) = 0.20$  (1)Ca +  $0.33$  (1)Na. Amplitudes and phases for the density waves:  $A_{M(1)}^p = 0.44$  (4),  $\varphi_{M(1)}^p = 0.95$  (1),  $A_{M(2)}^p = 0.42$  (3),  $\varphi_{M(2)}^p = 0.44$  (1).

	$x$	$y$	$z$	$U_{\text{eq}}$	$A^x$	$A^y$	$A^z$	$\varphi^x$	$\varphi^y$	$\varphi^z$
$M(1)$	2673 (1)	9799 (1)	831 (1)	27	4 (1)	8 (1)	3 (1)	83 (1)	45 (1)	80 (1)
$M(2)$	2718 (1)	277 (1)	513 (1)	15	2 (1)	1 (1)	3 (1)	88 (2)	76 (1)	47 (1)
$T_1(O)$	67 (1)	1651 (1)	1067 (1)	13	5 (1)	6 (1)	2 (1)	95 (3)	48 (1)	30 (4)
$T_1(M)$	37 (1)	8176 (1)	1160 (1)	11	5 (1)	6 (1)	-1 (1)	47 (3)	50 (1)	25 (5)
$T_2(O)$	6868 (1)	1093 (1)	1586 (1)	11	3 (1)	4 (1)	1 (1)	79 (4)	94 (2)	49 (6)
$T_2(M)$	6822 (1)	8796 (1)	1786 (1)	11	4 (1)	5 (1)	0 (1)	44 (3)	95 (2)	24 (8)
$OA(1)$	27 (1)	1295 (1)	4887 (1)	20	5 (2)	8 (1)	1 (1)	37 (6)	1 (2)	8 (25)
$OA(2)$	5836 (1)	9936 (1)	1389 (1)	13	4 (2)	5 (1)	1 (1)	59 (8)	3 (3)	58 (26)
$OB(O)$	8128 (1)	1067 (1)	951 (1)	18	5 (2)	3 (1)	-1 (1)	84 (6)	51 (6)	84 (12)
$OB(M)$	8176 (1)	8526 (1)	1237 (1)	25	8 (2)	0 (1)	5 (1)	47 (4)	0 (34)	67 (4)
$OC(O)$	149 (1)	2936 (1)	1387 (1)	16	7 (2)	7 (1)	2 (1)	1 (4)	41 (2)	30 (8)
$OC(M)$	166 (1)	6887 (1)	1087 (1)	16	8 (2)	7 (1)	3 (1)	52 (4)	46 (2)	92 (7)
$OD(O)$	1989 (1)	1084 (1)	1924 (1)	15	7 (2)	6 (1)	1 (1)	16 (4)	52 (3)	19 (13)
$OD(M)$	1887 (1)	8669 (1)	2152 (1)	18	4 (2)	4 (1)	1 (1)	73 (7)	55 (4)	83 (14)

scattering factors and anomalous-dispersion corrections were taken from *International Tables for X-ray Crystallography* (1974).

### Results and discussion

The atomic coordinates, equivalent isotropic temperature factors and modulation parameters are listed in Table 2.\* An interpretation of the modulation of the framework will be given below based on an analysis of the average  $T$ -O distance functions. Following Ribbe & Gibbs (1969) the percentage Al content of the  $T$  sites will be evaluated by the formula  $\text{Al}/(\text{Al} + \text{Si}) = 658(\langle T-O \rangle - 1.605)$ .

A comparison of the results for  $An_{38}$  and  $An_{52}$  (Yamamoto *et al.*, 1984) shows similar modulation principles but lower amplitudes for  $An_{38}$ . This corresponds to the lower average intensity of the  $e$  reflections for  $An_{38}$  and can be explained in the way in which the structural differences between the antiphase domains vanish progressively with decreasing An content. This could take place in purely displacively modulated structures by decreasing the amplitudes and retention of perfect order. For the  $e$ -plagioclases, however, the shift modulation is solely a consequence of the Al/Si substitutional modulation, and smaller amplitudes of the density waves imply a more statistical distribution of Al and Si on the  $T$  sites connected with higher structural disorder of the framework atoms.

\* Lists of structure factors and anisotropic thermal parameters have been deposited with the British Library Document Supply Centre as Supplementary Publication No. SUP 44791 (18 pp.). Copies may be obtained through The Executive Secretary, International Union of Crystallography, 5 Abbey Square, Chester CH1 2HU, England.

Fig. 5 shows the Al/Si substitutional modulation of the characteristic building element of the plagioclases as defined by Wenk & Kroll (1984). The Ab- and An-like elements (composition for  $An_{100}$ :  $\text{AlSi}_3$  and  $\text{Al}_3\text{Si}$ ) have in our case the composition  $\text{Al}_{1.05}\text{Si}_{2.95}$  and  $\text{Al}_{1.5}\text{Si}_{2.5}$ . The An-like group has been largely assimilated to the Ab-like group. This confirms the statement of Wenk & Kroll (1984) concerning the incorporation of Si/Na into intermediate plagioclases.

Naturally, the compositions of the Ab- and An-like groups found can be realized in a statistical manner only. Phase fluctuations can be excluded as a possible cause and must be small otherwise both groups would show chemical formulas that deviate from  $\text{AlSi}_3$  and  $\text{Al}_3\text{Si}$  [we always assume the validity of Loewenstein's rule (Loewenstein, 1954)]. A possible explanation could be that the crystal exhibits domains with the antiphase structure  $An \dots An^*$  which are separated by Ab regions. The superposition of the coherent-scattering structures of the domains and the Ab regions would not change the composition of an Ab-like group but would that of an An-like building element. Indeed electron microscope images indicate that the APB structure is coherent over areas of  $< 1000 \text{\AA}$  which are separated by regions with  $C\bar{1}$  structure (Grove, Ferry & Spear, 1983). The results of the refinements with individual scale factors for the satellites mentioned above support this model in principle. The very high correlations, however, between the satellite scale factor and the modulation amplitudes do not allow reliable confirmation of the model.

### M-ordering

The  $M$  site of the  $e$ -plagioclases must always be described by a split-atom model. The electron-density maps of this site do not show essential differences for plagioclases with compositions from  $An_{28}$  to  $An_{66}$  (Smith, 1984). The relative Ca/Na distribution over the

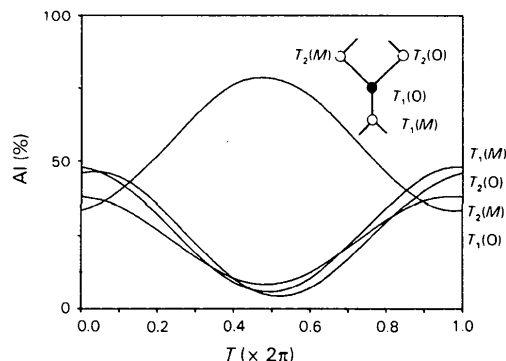


Fig. 5. The variation of the Al content of the  $T$  sites of a characteristic building element (shown in the insert) of the  $e$ -plagioclases derived from  $T$ -O distances. For comparison the values of the average structure of  $An_{38}$  are:  $T_1(O)$  57%Al,  $T_1(M)$  26%Al,  $T_2(O)$  24%Al and  $T_2(M)$  26%Al.

split sites should therefore be independent of the Ca content though the split site  $M(2)$  is preferentially occupied by Ca (Gerald, Parise & Mackinnon, 1986). In any case, the degree of occupation of one of the split positions is strongly correlated with the modulation of the framework. In the regions with strong antiphase relation (An and An\*) opposite split sites are occupied whereas in the boundary zones the distribution found in the average structure exists. Fig. 6 represents the  $M$ -site ordering in sections through the (3+1)-FF. Both split positions are occupied in varying amounts during a modulation period. The overall occupancy of the  $M$  site remains constant in contrast to  $An_{52}$  where a slight

density modulation ( $A_{Ca}^p = A_{Na}^p = 0.2$ ) has been found (Yamamoto *et al.*, 1984).

The existence of  $f$  reflections in the calcic intermediate plagioclases can be explained only in the way proposed in the KM or HTKJ models, namely by a sequence of Ab- (or labradorite-) and An-like lamellae. The labradorite  $An_{52}$  with its weak  $f$  reflections seems to represent the lower boundary for the applicability of this model. The more sodic plagioclases which also show different physical properties and smaller modulation periods are characterized by the condensation of the Ab part in regions between domains with An...An\* structure. The averaging X-ray structure analysis therefore yields a homogenous Ca/Na distribution over the  $M$  site. According to Kitamura & Morimoto (1984) the modulated structure of the  $e$ -plagioclases is stabilized by resonance between a Ca-rich  $I$ -An and a Na-rich  $I$ -Ab, whereby the  $I$ -Ab is formed by ordering of the Na on the  $M$  split sites. In the sodic plagioclases we do have  $I$ -structural elements but no  $I$ -Ab ones. Therefore no resonance is possible. Possibly, this one is of the reasons for the higher stability (Carpenter, 1986) of the calcic plagioclases.

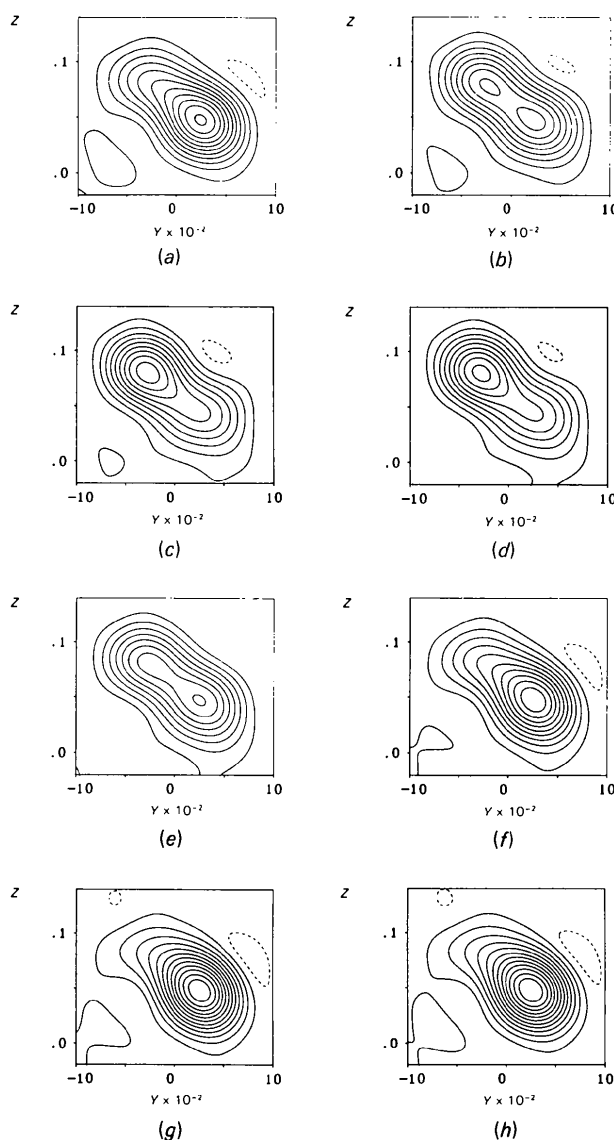


Fig. 6. Sections through the (3+1)-FF of  $An_{38}$  around the  $M$  site parallel to  $yz$  with (a)  $t=0$ , (b)  $t=0.125$ , (c)  $t=0.25$ , (d)  $t=0.375$ , (e)  $t=0.5$ , (f)  $t=0.625$ , (g)  $t=0.75$  and (h)  $t=0.875$ .

### Real structure

As mentioned above, the modulated structure contains a considerable amount of disorder which is essentially associated with the  $M$  sites. Two possible explanations may be given for this case:

(a) The Ca/Na distribution is random, the split positions being determined by the Al/Si distribution in the surrounding Si/Al tetrahedra.

(b) There is an ordering process of Ca/Na following another structural principle, having a minor correlation with the Si/Al-ordering process. Because of the repulsive forces between cations of equal charges there must be a general ordering force avoiding Ca-Ca pairs as nearest neighbours. These interactions would favour superstructure formation. Obviously, the closest distances between  $M$  sites lie very near to the  $ac$  plane.

There are also two possible reasons for short-range ordering:

(a) Formation of a superstructure in the  $ac$  plane should result in diffuse maxima in, or near to the reciprocal plane ( $h0l$ ). This is not observed on strongly overexposed diffraction pictures.

(b) If the ordering process takes place without a change of cell dimensions, then we must expect a noncentrosymmetric cation distribution function. The diffuse scattering should be observed in the neighbourhood of the  $a$  reflections.

It is well known that anomalies are observed near to the  $a$  reflections, namely the supersatellites reported by Jagodzinski & Korekawa (1965) and very weak satellites, observed by Jagodzinski & Penzkofer (1981). The observation that the supersatellites have a  $q$  vector

nearly parallel to the  $b^*$  direction supports the possibility of lamellar cation ordering in the  $ac$  plane. Then the modulated structure (let us call this an  $s$ -modulated structure) should be generated by two types of domains which are centrosymmetric to each other. Both the  $e$ - and  $s$ -modulated structures are incommensurate to each other in a first approximation. In this particular case, structure determination of only one of the modulated structures reveals the ordering process of the second as random. Hence, a random distribution for Ca/Na will be derived in a structure determination. There are other experimental observations which support this model:

(a) Intensity calculation of the  $s$ -modulated structure (Jagodzinski & Penzkofer, 1981) yields main reflections whose intensities are given by

$$I(hkl) \propto \frac{1}{2} |F(hkl)| \exp[i\varphi(hkl)] \\ + \frac{1}{2} |F(hkl)| \exp[-i\varphi(hkl)]|^2 \\ = |F(hkl)|^2 \cos^2 \varphi(hkl)$$

where  $\varphi(hkl)$  is the phase factor of the noncentrosymmetric structure. On the other hand, the intensities of the  $s$  satellites are given by

$$I_s(hkl) \propto \langle |F(hkl)|^2 \rangle - |\langle F(hkl) \rangle|^2 \\ = |F(hkl)|^2 \sin^2 \varphi(hkl)$$

As long as the phases of the noncentrosymmetric structure are below  $2\pi/8$  the satellites have a lower intensity than the main reflections. This agrees well with the experimental observation of satellite intensities which are occasionally comparable with those of the main reflections.

(b) The supersatellites near  $(0k0)$  main reflections are absent or so weak that they could not be observed (Korekawa & Jagodzinski, 1967). This experimental fact supports the conclusion of an ordering process in the  $(0k0)$  plane, as all displacements within this plane cannot be detected in  $(0k0)$  reflections. Further, this 'extinction rule' excludes an important density effect in the  $s$ -modulated structure.

Apparently, the model discussed above is far too crude to give a detailed explanation of the complicated diffraction patterns of the plagioclases. One of the most important alterations to be introduced is the correlation between Si/Al and Ca/Na ordering. Since both ordering processes generate electrical fields, these may influence the orientation of the lamellar planes. It seems inappropriate in the present state of structure research of plagioclases to enter a detailed discussion without further experimental information. Some remarks, however, should be given on how to obtain a correct solution of the disorder problem of plagioclases. The following procedures have to be performed in order to arrive at reliable results:

(a) The real average structure has to be determined by separating the  $s$ -satellites near to the main reflec-

tions. All structure investigations of plagioclases use integrated intensities. This integration may to some extent exclude the disorder indicated by the  $s$  satellites. Unfortunately, this statement can only be true if all main reflections are accompanied by satellites with an intensity comparable to the main reflections. This is in clear disagreement with the experimental results. Hence, a determination of the *real* average structure is necessary which should yield important new information on the displacement vectors, and specifically the  $M$  positions.

(b) Following the procedure described above, a solution of the  $s$ -modulated structure has to be performed. This would yield the necessary information on the ordering processes and their correlations.

(c) It is obvious that the  $e$ -modulated structure must be different in the two types of  $s$  domains; hence, the structure determination of the  $e$ -modulated structure has to start with the assumption of two different structures. Unfortunately, no separation of the  $e$  satellites has been observed so far which would allow incoherent refinement of the two  $e$ -modulated structures. On the other hand, no splitting of  $e$  satellites could be detected, even in photographs with a very high resolution (Korekawa & Jagodzinski, 1967). Hence, it is impossible to determine an average structure for the two  $e$ -modulated structures. The results of refinements with intensity integration are very doubtful for the same reasons as discussed above for the  $s$  satellites.

(d) It should be stressed that the ordering process for  $s$  domains does not necessarily need to be lamellar in its character. Irregularly shaped domains hamper the determination of the ordering processes, but do not preclude a determination of the average structure. In this case, the intensity of satellites is smeared around  $a$  reflections and may well be separated from the sharp  $a$  reflections.

The mistake made in previous structure determinations of plagioclases was the assumption of an 'unmixing' process into albite and anorthite lamellae and a strict coupling of the ordering process of Al/Si and Ca/Na. New structural models have to be based on experiments with high-resolution power, exceeding the possibilities of conventional diffractometers. Renewed experiments with synchrotron radiation may provide a means to overcome this difficulty in an adequate manner.

We thank H. R. Wenk for making the crystal Vz433a available to us.

#### References

- CARPENTER, M. A. (1986). *Phys. Chem. Miner.* **13**, 119–139.  
 FRENZ, B. A. (1978). *The Enraf-Nonius CAD-4 SDP - A Real-Time System for Concurrent X-ray Data Collection and Crystal Structure Solution*. In *Computing in Crystallography*, edited by H. SCHENK, R. OLTJOF-HAZEKAMP, H. VAN KONINGSVELD & G. C. BASSI. Delft Univ. Press.

- GERALD, J. D. F., PARISE, J. B. & MACKINNON, I. D. R. (1986). *Am. Mineral.* **71**, 1399–1408.
- GROVE, T. L., FERRY, J. M. & SPEAR, F. S. (1983). *Am. Mineral.* **68**, 41–59.
- HORST, W., TAGAI, T., KOREKAWA, M. & JAGODZINSKI, H. (1981). *Z. Kristallogr.* **157**, 233–250.
- International Tables for X-ray Crystallography* (1974). Vol. IV. Birmingham: Kynoch Press. (Present distributor Kluwer Academic Publishers, Dordrecht.)
- JAGODZINSKI, H. (1984). *Bull. Mineral.* **107**, 455–466.
- JAGODZINSKI, H. (1986). Personal communication.
- JAGODZINSKI, H. & KOREKAWA, M. (1965). *Naturwissenschaften*, **52**, 640–641.
- JAGODZINSKI, H. & PENZKOFER, B. (1981). *Acta Cryst.* **A37**, 754–762.
- KITAMURA, M. & MORIMOTO, N. (1975). *Proc. Jpn Acad.* **51**, 419–424.
- KITAMURA, M. & MORIMOTO, N. (1977). *Phys. Chem. Miner.* **1**, 199–212.
- KITAMURA, M. & MORIMOTO, N. (1984). *Feldspars and Feldspathoids. Structures, Properties and Occurrences*, NATO–ASI Ser. C, Vol. 137, edited by W. L. BROWN, pp. 95–120. Dordrecht: D. Reidel.
- KOREKAWA, M. & JAGODZINSKI, H. (1967). *Schweiz. Mineral. Petrogr. Mitt.* **47**, 91–100.
- LOEWENSTEIN, W. (1954). *Am. Mineral.* **39**, 92–96.
- NAKAJIMA, Y., MORIMOTO, N. & KITAMURA, M. (1977). *Phys. Chem. Miner.* **1**, 213–225.
- OVERHAUSER, A. W. (1971). *Phys. Rev. B*, **3**, 3173–3182.
- RIBBE, P. H. (1983). *Reviews in Mineralogy*, Vol. 2, *Feldspar Mineralogy*. Washington, DC: Mineralogical Society of America.
- RIBBE, P. H. & GIBBS, G. V. (1969). *Am. Mineral.* **54**, 85–94.
- SMITH, J. V. (1984). *Feldspars and Feldspathoids. Structures, Properties and Occurrences*, NATO–ASI Ser. C, Vol. 137, edited by W. L. BROWN, pp. 55–94. Dordrecht: D. Reidel.
- SMITH, J. V. & WENK, H. R. (1983). *Am. Mineral.* **68**, 742–743.
- STEURER, W. (1987). *Acta Cryst.* **A43**, 36–42.
- STEURER, W. & ADLHART, W. (1983). *Acta Cryst.* **B39**, 349–355.
- TOMAN, K. & FRUEH, A. J. (1976a). *Acta Cryst.* **B32**, 521–525.
- TOMAN, K. & FRUEH, A. J. (1976b). *Acta Cryst.* **B32**, 526–538.
- WENK, H. R., JOSWIG, W., TAGAI, T., KOREKAWA, M. & SMITH, B. K. (1980). *Am. Mineral.* **65**, 81–95.
- WENK, H. R. & KROLL, H. (1984). *Bull. Mineral.* **107**, 467–487.
- WOLFF, P. M. DE (1974). *Acta Cryst.* **A30**, 777–785.
- YAMAMOTO, A., NAKAZAWA, H., KITAMURA, M. & MORIMOTO, N. (1984). *Acta Cryst.* **B40**, 228–237.

*Acta Cryst.* (1988). **B44**, 351–355

## The Ferric Ion Distribution and Hydrogen Bonding in Epidote: a Neutron Diffraction Study at 15 K

BY ÅKE KVICK

*Chemistry Department, Brookhaven National Laboratory, Upton, NY 11973, USA*

AND JOSEPH J. PLUTH, JAMES W. RICHARDSON JR AND JOSEPH V. SMITH

*Department of Geophysical Sciences and Materials Research Laboratory, The University of Chicago, Chicago, Illinois 60637, USA*

(Received 21 September 1987; accepted 23 February 1988)

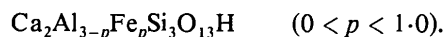
### Abstract

The crystal structure of epidote,  $\text{Ca}_2\text{Al}_{2.2}\text{Fe}_{0.8}\text{Si}_3\text{O}_{13}\text{H}$ , at 15 K,  $M_r = 477.5$ ,  $P2_1/m$ ,  $a = 8.893$  (2),  $b = 5.630$  (3),  $c = 10.150$  (2) Å,  $\beta = 115.36$  (1)°,  $V = 459.2$  Å<sup>3</sup>,  $Z = 2$ ,  $D_m = 3.482$  g cm<sup>-3</sup>,  $\mu = 0.186$  cm<sup>-1</sup>, was determined at the Brookhaven National Laboratory High Flux Beam Reactor using a neutron wavelength of 1.15948 (12) Å. 2409 reflections were used in least-squares refinement resulting in a final  $R(F^2)$  of 0.0246 and  $wR(F^2) = 0.0331$ . Anharmonic displacement tensors of up to order four for the H atom were refined. The analysis assigned 0.757 (3) Fe<sup>3+</sup> ions to the larger octahedral site and 0.015 (3) Fe<sup>3+</sup> to one of the other octahedral sites. The H atom is uniquely located on the O(10) atom with a bonding distance of 0.975 (1) Å and is involved in a bent hydrogen bond to O(4) [O(10)···O(4) 2.922 (1), H···O(4) 1.964 (1) Å, O(10)–H···O(4) 166.9 (1)°]. The bending of the bond

is associated with the electrostatic repulsion from the Fe<sup>3+</sup> [Fe···H 2.728 (1) Å] and Ca<sup>2+</sup> ions [Ca(2)···H 3.0043 (14) Å]. The Fe/Al interchange in the octahedral site causes some structural reorganization, primarily a rotation of the Si(2) tetrahedron around its central atom and changes in the hydrogen-bond geometry.

### 1. Introduction

The epidote group of minerals, a common and complex family of rock-forming silicates, raises unresolved challenges to petrologists, chemists and geophysicists. The group may be represented by the chemical formula



Fe<sup>3+</sup> ions substitute for Al in this range and the different minerals are commonly referred to as zoisite or clinozoisite (orthorhombic and monoclinic) for low Fe